Sediment flux from the morphodynamics of elongating linear dunes

Antoine Lucas[1]*, Clément Narteau[2], Sébastien Rodriguez[1], Olivier Rozier[2], Yann Callot[3], Amandine Garcia[1], and Sylvain Courrech du Pont[4]

[1]Laboratoire Astrophysique, Instrumentation et Modélisation, UMR 7158 CNRS, Université Paris-Diderot, CEA Saclay, Gif-sur-Yvette, France
[2]Institut de Physique du Globe de Paris, Sorbonne Paris Cité, Université Paris Diderot, UMR 7154 CNRS, Paris, France
[3]Laboratoire Archorient-Environnements et Sociétés de l'Orient Ancien, UMR 5133 CNRS, Université Lumière Lyon 2, Lyon, France
[4]Laboratoire Matière et Systèmes Complexes, Sorbonne Paris Cité, Université Paris Diderot, UMR 7057 CNRS, Paris, France

ABSTRACT

Although dunes are very common bedforms in terrestrial sand seas, the description of linear dune growth, either by extension or lateral accretion, is still hindered by our limited understanding of the underlying mechanisms. Therefore, sand flux estimates from remote imagery rely essentially on the migration speed of barchan dunes, but not on the dynamics of linear dunes. Here we use ~50 yr of high-resolution aerial and satellite imagery of the Ténéré desert (Niger), the world's largest source of mineral aerosols, to demonstrate that linear dunes can elongate in the direction of the resultant sand flux with no lateral migration. As they elongate from topographic obstacles in a zone of low sediment availability with multimodal winds, these elongating lee dunes are ideal to isolate and quantify linear dune growth only by extension. Using similar conditions in a numerical model, we show how deposition downstream of low hills may result in nucleation and development of bedforms. From elongation we derive the local sand flux parallel to the linear dune crests. This study shows that the morphodynamics of linear dunes under complex wind regimes can also be used for assessing sediment flux and wind conditions, comparably to the more-established method of using sand flux estimates perpendicular to the barchan dune crests in zones of unidirectional wind.

INTRODUCTION

Linear dunes are the most common dune type in sand seas exposed to multidirectional wind regimes (Pye and Tsoar, 1990). Their morphology may vary in size, sinuosity, and aspect ratio, but they are all characterized by long ridges capable of extending over tens of kilometers. Dunes are classified according to the angle, φ, between their crest orientation and the direction of the resultant sand flux (Hunter et al., 1983), and are usually identified as transverse (φ > 75), oblique (15 < φ < 75), or longitudinal (φ < 15). The role of lateral accretion is evident in transverse and oblique dunes development, as they can grow in height from the sediment of the interdune and/or migrate by recycling their own sediment through the normal-to-crest components of transport (Rubin and Hunter, 1987; Ping et al., 2014). For longitudinal dunes, also referred to as seif dunes (Tsoar, 1982) or silks (Mainguet and Callot, 1978), the contribution of the parallel-to-crest components of transport is not negligible, so that dunes may also grow by extension through deposition at the dune tip in the direction of the resultant sand flux (Tsoar, 1982, 1989; Tsoar et al., 2004; Telfer, 2011). There was no consensus in the past regarding the underlying dynamical processes of eolian bedforms (Bagnold, 1941; Tsoar, 1983), and it is only recently that two distinct dune growth mechanisms have been proposed, based on laboratory and numerical experiments (Courrech du Pont et al., 2014; Gao et al., 2015). Depending on sand availability, these studies reveal that dunes either preferentially grow by extension for low sediment supply (i.e., the fingering mode, first illustrated by Reffet et al., 2010) or by lateral accretion for high sediment supply (i.e., the maximum gross bedform-normal transport of Rubin and Hunter, 1987). Most important, the prevailing growth mechanism selects the dune orientation, which can be analytically derived from the wind data and compared to observations in the field (Courrech du Pont et al., 2014).

Previous studies have generally used winds external to the dunes to calculate the sand transport vectors that are used to classify dunes by orientation (Rubin and Hunter, 1987). However, some researchers have noted that the dunes influence the overall transport direction due to deflection of flow (Tsoar, 1983) or due to dune aspect ratio, and speed-up over dune flanks (Zhang et al., 2012; Courrech du Pont et al., 2014). Here we follow the approach in Courrech du Pont et al. (2014), and quantify the sand transport according to the feedback of dune morphology on the magnitude of the flow: under a multidirectional wind regime, each wind encounters different dune aspect ratios, and consequently the resultant sand transport vector on the dunes differs from the resultant sand transport vector external to the dunes.

There are only a few, limited studies of the dynamics of linear dunes (Rubin and Hunter, 1985; Bristow et al., 2000; Tsoar et al., 2004; Rubin et al., 2008; Ping et al., 2014), and most of the quantitative understanding relies on ground-penetrating radar analysis coupled with luminescence dating (Bristow et al., 2007a, 2007b; Telfer, 2011). In previous studies, it was shown that in-dividual dunes simultaneously elongate and migrate laterally. Combined evolution by elongation and migration is not surprising given the natural fluctuations of the terrestrial wind regimes and the complex dune interactions in the field (e.g., collisions, pattern coarsening). However, as soon as the dunes migrate laterally, a dominant dip associated with lateral accretion prevails in the sedimentary structure. This may explain why dune elongation has not been analyzed as a major agent in the formation of dune fields.

We take advantage of interactions between small-scale topographic obstacles and sediment transport to quantitatively study how dunes can nucleate and grow by only extension over long distances with an orientation that remains parallel to the resultant sand flux at the crest. Using such a special case of lee dunes, for which the elongation flux can be separated from the lateral migration flux, we propose a methodology for estimating sand flux from the morphodynamics of linear dunes.

We analyze the dune patterns of the Erg of Fachi-Bilma, the eastern part of the Ténéré desert in Niger (Fig. 1). As in the entire east-central Sahara, this region is exposed to the Harmattan, a dry southeasterly trade wind, which is particularly strong in winter. From southern Libya to northern Mali, hyperarid climate and low sand availability provide ideal conditions to characterize transitions in dune types (Clos-Arceduc, 1969; Wilson, 1971; Gao et al., 2015), as well as the effect of topography on large-scale atmospheric circulations and the subsequent sand flow paths (Mainguet and Callot, 1978). The Harmattan is topographically steered by various mountain ranges. As the near-surface winds are diverted and channelized, they vary strongly in strength and orientation along the different airflow paths. Downwind of the corridor between the Tibesti and the Ennedi massifs, the best known example is the easterly low-level jet blowing over the Bodélé depression in central Chad, one of the principal sources of dust in the world (Washington et al., 2006), where 20-m-high barchan dunes propagate at a speed of 50 m/yr (Vermeesch and Leprince, 2012). In the wake of the Tibesti Mountains, there is a clear bimodal wind regime with a strong peak from the northeast and a weaker peak from the southeast with a divergence angle of 75° (Fig. 1). In this area linear dunes in the alignment of the re-
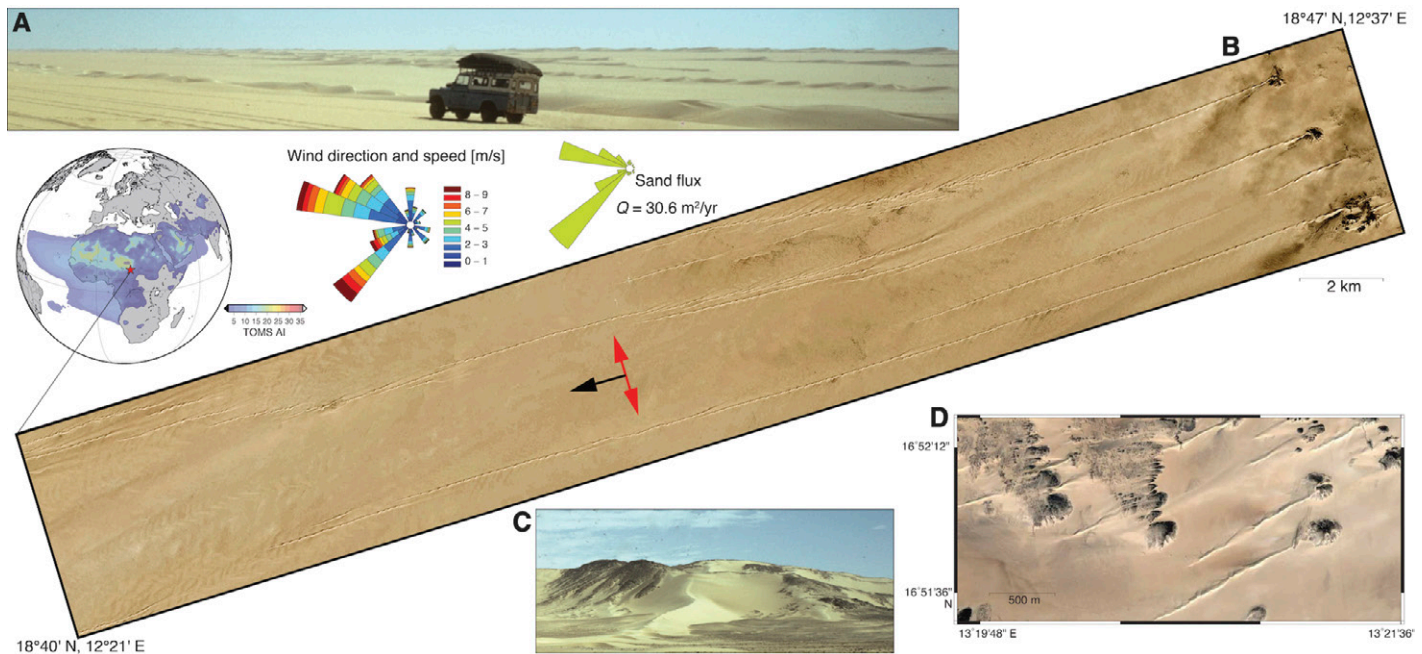
Figure 1. A–D: Elongating dunes in the Erg of Fachi-Bilma, Niger. Lateral and top view pictures of the dune field are at different length scales. Linear dunes grow from the lee slope of residual hills, keeping constant orientation with well-defined width and height over tens of kilometers. Wind and sand roses external to the dunes are calculated from the Bilma airport data from 2000 to 2013 (18°41′N, 12°55′E). Black and red arrows in B show the predicted dune trend in the fingering and bed instability modes, respectively. The globe shows the Total Ozone Mapping Spectrometer aerosol index (TOMS AI) (Washington et al., 2006).

sultant sand flux are generally attached to topographic obstacles such as residual hills (Fig. 1). Sinuous crest lines grow directly from these lee dunes, and keep a constant orientation for a considerable distance (>10 km).

DATA AND METHODS

In order to study dune morphodynamics, we collected satellite images from Landsat, ASTER (Advanced Spaceborne Thermal Emission and Reflection Radiometer), and Google Earth™ (including Spot and GlobalView data), as well as aerial images taken in 1957 by IGN (Institut Geographique National, France) (Mainguet and Callot, 1978). We complete this data set with a Pléiades satellite stereo pair we acquired during the fall of 2014. Using photogrammetric solutions, we derive a three-dimensional (3-D) point cloud with a submeter ground sampling and a vertical accuracy close to 1 m (Fig. 2A; see the GSA Data Repository[1]). We generated a digital surface model (DSM) over a regular grid with a spacing of 4 m. Note that, because dune heights do not exceed a few meters (Fig. 2), our DSM is

the only remote-sensing data set available that can resolve the 3-D morphology of the dunes, since no in-situ topographic survey has been done. Eventually, the entire data set of satellite imagery and the DSM will be coregistered so that we can assess the detection of change with a metric resolution.

RESULTS

Our analysis shows that, from 1957 to 2014, the linear dunes did not consistently migrate laterally, but systematically grew by extension with a remarkable regularity (Fig. 2). Stacking a large number of cross-section profiles along individual dunes, the DSM shows that they keep constant height and width over the growing tip (i.e., the last 100 m). The dune tip heights range from 1 to 6 m. This narrow dispersion suggests that all the elongating dunes are morphologically and dynamically similar. Upstream, the dune body may be significantly thicker, to 10 m high and 60 m wide, keeping an aspect ratio (height divided by half-width) of ~0.3 ± 0.05 (Fig. 2) across the entire dune field.
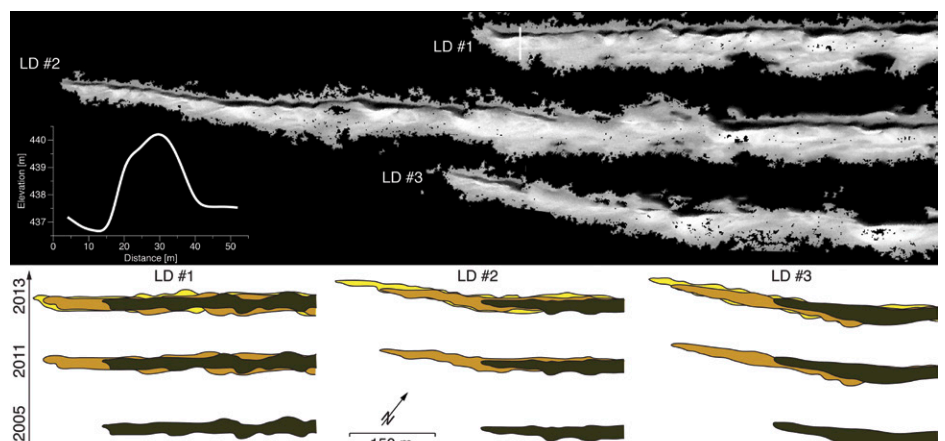

Figure 2. Morphodynamics of linear dunes from satellite imagery. A: Three-dimensional point cloud map derived from Pléiades stereo pair (18°37′55″N, 12°44′04″E). The inset shows a topographic cross-section profile and the corresponding point cloud at the termination of linear dune 1 (LD #1). B: Evolution of dune shape from July 2005 to March 2013 (for examples over longer time periods, see the Data Repository [see footnote 1]).

While the dune tips propagate on a nonerodible bed, dune bodies remain at the same position (see the Data Repository). Dune flanks are continuously reshaped by the development and propagation of transverse superimposed bedforms, which produce sinuous crestlines and intermittent avalanche faces. From all the available time series, we measured 80 individual elongation rates for 25 dunes over different time periods and found a mean elongation rate value of 20 ± 10 m/yr (Fig. 3).

The lateral stability of dunes indicates that they keep the alignment for which the normal-to-crest components of transport cancel each other out. These results show that dunes grow only by extension in the direction of the resultant sand flux at the crest. This resultant sand flux, Q_{dune}, can be directly derived from the elongation rate e and dune shape considering the equation of conservation of mass over the entire cycle of wind reorientation: $Q_{dune} = e(S/W)$, where S and W are the cross section and the width of the dune perpendicular to dune crest, respectively (Figs. 2 and 3). Where the exact dune morphology cannot be derived from the bed elevation profile, we extrapolate the dune aspect ratio accounting for the measured width, hence the resultant sand flux can be derived from $Q_{dune} = A \times eW$, where A is proportional to the dune aspect ratio and the corresponding cross section (see the Data Repository).

Figure 3 shows that, in the Erg of Fachi-Bilma, $Q_{dune} = 28^{+22}_{-10}$ m²/yr. This value can be compared to the one derived from the wind data using the transport law of Ungar and Haff (1987) with a threshold shear velocity of 19 cm/s for the entrainment of 180 μm sand grains (i.e., the D_{50} measured in the field; see the Data Repository). These calculations lead to resultant sand fluxes of 22.6 and 39.2 m²/yr away from the dunes and at the dune crests, respectively, fully consistent with the value of Q_{dune} determined from the imagery. The differences between these fluxes can be used to estimate the loss of sediment at the dune tip during periods of constant wind direction, together with the wind speed-up at the dune crests.

DISCUSSION

In this zone of low sand availability, pure dune elongation is observed as a result of topographic obstacles that allow nucleation and extension of linear bedforms from the lee-side accumulation of sediment transported from upwind. To investigate these interactions between sand flux and topographic obstacles and generalize our observation to all linear dunes, we use a cellular automaton dune model that accounts for feedback mechanisms between the flow and the evolving bed topography (Narteau et al., 2009; see the Data Repository). When the sediment input rate is smaller than the transport capacity of the wind, the simulations show that no bedform develops on a flat nonerodible ground. In contrast, obstacles generate zones of deposition on the lee slopes (Fig. 4A). Exposed to 2 asymmetric winds with a divergence angle of 75° and a transport ratio of 1.5 corresponding to the wind regime of the Erg of Fachi-Bilma, these zones of sediment accumulation do not develop as sand shadows (Bagnold, 1941), but produce finger-like structures that extend far away from the source (Fig. 4B). As observed in the field, linear dunes in the simulations grow only by extension from the resultant sand flux at the crest, which is parallel to the dune alignment. The extension rates predicted by the model are the same order of magnitude as the measured ones (green squares in Fig. 3). Because of the
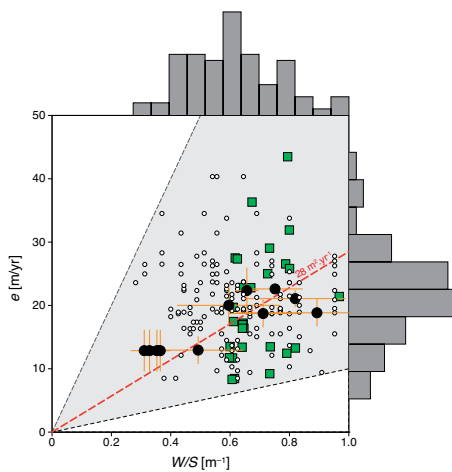

Figure 3. Sediment flux estimation from the elongation rate *e* and the linear dune shape (*W/S*, where *W* and *S* are the width and the cross section, respectively). Black dots show the elongation rate with respect to dune shape for linear dunes that are covered by the digital surface model (DSM). White dots are measurements for which the cross section is derived from dune width using the scaling obtained from the DSM (see the Data Repository [see footnote 1]). Histograms show the distributions of elongation rate and dune shape. The resultant sand flux ranges from 15 to 55 m²/yr (black dashed lines) with a mean value of 28 m²/yr (red dashed lines). Error bars in dune height are the standard deviation of at least 10 transects at the dune tip (see Fig. 2A). Error bars in elongation rate are estimated to be ~10% of the measured values. Green squares are the results from numerical simulation shown in Figure 4.
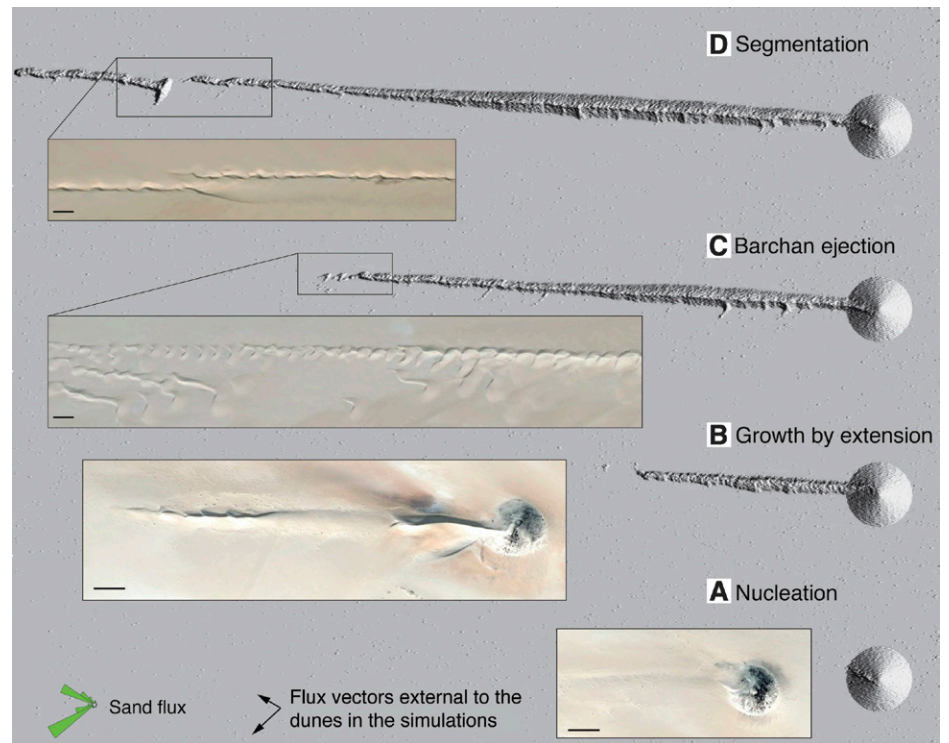

Figure 4. Topography-driven dune morphodynamics from numerical modeling. A constant sediment injection rate Q_{in} = 7.5 m²/yr is maintained upstream of a flat nonerodible ground. As in the Erg of Fachi-Bilma (Niger), the saturated flux, Q_0, is equal to 30.6 m²/yr and the bidirectional wind regime has a divergence angle of 75° and a transport ratio of 1.5 between the 2 winds. A: Nucleation of bedforms in the deposition zone downstream of the topographic obstacle (see the Data Repository [see footnote 1]). B: Linear dune growth by extension from the lee dune. C: Development of transverse superimposed bedforms and ejection of barchans. D: Segmentation and ejection of linear dunes. Meanwhile they continue to grow by extension and migrate laterally in the direction of the resultant flux external to the dunes (i.e., the direction of the sum of the black sand transport vectors). Insets from the Erg of Fachi-Bilma show similar behaviors. Black scale bars = 100 m.

development of transverse superimposed bedforms, smaller barchans may be ejected and propagate away from the linear dune. This essentially happens at the dune tip, as observed in both the simulations and the field, from satellite imagery (Fig. 4C). Secondary dune features can also reach the height of the main structure to break it into a set of new linear dunes (Fig. 4D). Once these segmented dunes are disconnected from the fixed source, the upstream end of the dune takes the form of a smooth sand hill (Fig. 4D). Such an isolated bedform is free to migrate laterally in the direction of the resultant sand flux at the crest (Ping et al., 2014). Then, the entire linear dune moves sideways while it continues to grow by extension in the resultant drift direction. Ultimately, it may generate several parallel linear dunes that interact with each other. All these features can be easily identified in the field across the Ténéré (Figs. 1 and 4) and in many other sand seas where both lateral migration and elongation have been identified in sedimentary records (Tsoar, 1982; Rubin and Hunter, 1985; Bristow et al., 2000; Telfer and Hesse, 2013). In many cases, there is no need of topography to produce linear dunes; they may simply arise from reshaping of other dune types or from accumulation of segregated fine grains. However, topographic obstacles and the associated upstream deposition zone generate fixed sources of sediment from which the linear dune can grow by elongation only.

Although flow deflection over the dune flanks may affect the final dune shape, our numerical results show that growth by extension requires neither transverse secondary flow nor migration of meandering waveform. Instead, elongation in the model results only from deposition at the dune termination in the direction of the resultant sand flux at the crest. In addition, our study provides practical solutions for the management of terrestrial dune fields by helping to predict the shape, direction, and velocity of active linear dunes, including these in presence of vegetation or cohesion, which are known to stabilize bedforms (Rubin and Hesp, 2009; Telfer, 2011). In some aspects, vegetated linear dunes may be analogous to the linear dunes studied here because their vegetated part can be considered as a natural topographic obstacle acting as a sand trap, from where the rest of the dune can undergo elongation only. The particularity of these bedforms is that the zone of deposition is not fixed and may expand along with the dune as the vegetation grows and occupies the newly formed parts of dunes. This may explain why, more than the other dune types, vegetated and/or cohesive dunes undergoing elongation are likely to exhibit straight or slightly sinuous ridges (Pye and Tsoar, 1990).

Combined with the systematic transverse instability of sand beds, dune elongation and lateral migration naturally explain the coexistence of dune patterns with different orientations, and can now be used for assessing sediment flux and surface wind conditions occurring in major sand seas on Earth as well as on Mars and Titan (Lucas et al., 2014).

REFERENCES CITED
Bagnold, R.A., 1941, The physics of blown sand and desert dunes: London, Methuen, 265 p.
Bristow, C.S., Bailey, S.D., and Lancaster, N., 2000, The sedimentary structure of linear sand dunes: Nature, v. 406, p. 56–59, doi:10.1038/35017536.
Bristow, C., Duller, G., and Lancaster, N., 2007a, Age and dynamics of linear dunes in the Namib Desert: Geology, v. 35, p. 555–558, doi:10.1130/G23369A.1.
Bristow, C., Jones, B.G., Nanson, G., Hollands, C., Coleman, M., and Price, D., 2007b, GPR surveys of vegetated linear dune stratigraphy in central Australia: Evidence for linear dune extension with vertical and lateral accretion, in Baker, G.S., and Jol, H.M., eds., Stratigraphic analyses using GPR: Geological Society of America Special Paper 432, p. 19–33, doi:10.1130/2007.2432(02).
Clos-Arceduc, A., 1969, Essai d'explication des formes dunaires sahariennes: Études de Photo Interprétation, v. 4, 66 p.
Courrech du Pont, S., Narteau, C., and Gao, X., 2014, Two modes for dune orientation: Geology, v. 42, p. 743–746, doi:10.1130/G35657.1.
Gao, X., Narteau, C., Rozier, O., and Courrech du Pont, S., 2015, Phase diagram of dune shape and orientation depending on sand availability: Scientific Reports (in press).
Hunter, R.E., Richmond, B.M., and Alpha, T.R., 1983, Storm-controlled oblique dunes of the Oregon coast: Geological Society of America Bulletin, v. 94, p. 1450–1465, doi:10.1130/0016-7606(1983)94<1450:SODOTO>2.0.CO;2.
Lucas, A., et al., 2014, Growth mechanisms and dune orientation on Titan: Geophysical Research Letters, v. 41, p. 6093–6100, doi:10.1002/2014GL060971.
Mainguet, M., and Callot, Y., 1978, L'Erg de Fachi-Bilma Tchad-Niger: Contribution à la connaissance de la dynamique des ergs et des dunes des zones arides chaudes: Memoires et Documents, Service de Documentation et de Cartographie Geographiques, Volume 19: Editions du Centre National de la Recherche Scientifique, 184 p.
Narteau, C., Zhang, D., Rozier, O., and Claudin, P., 2009, Setting the length and time scales of a cellular automaton dune model from the analysis of superimposed bed forms: Journal of Geophysical Research, v. 114, F03006, doi:10.1029/2008JF001127.
Ping, L., Narteau, C., Dong, Z., Zhang, Z., and Courrech du Pont, S., 2014, Emergence of oblique dunes in a landscape-scale experiment: Nature Geoscience, v. 7, p. 99–103, doi:10.1038/ngeo2047.
Pye, K., and Tsoar, H., 1990, Aeolian sand and sand dunes: London, Unwin Hyman, doi:10.1007/978-94-011-5986-9.
Reffet, E., Courrech du Pont, S., Hersen, P., and Douady, S., 2010, Formation and stability of transverse and longitudinal sand dunes: Geology, v. 38, p. 491–494, doi:10.1130/G30894.1.
Rubin, D., and Hesp, P.A., 2009, Multiple origins of linear dunes on Earth and Titan: Nature Geoscience, v. 2, p. 653–658, doi:10.1038/ngeo610.
Rubin, D., and Hunter, R., 1985, Why deposits of longitudinal dunes are rarely recognized in the geologic record: Sedimentology, v. 32, p. 147–157, doi:10.1111/j.1365-3091.1985.tb00498.x.
Rubin, D., and Hunter, R., 1987, Bedform alignment in directionally varying flows: Science, v. 237, p. 276–278, doi:10.1126/science.237.4812.276.
Rubin, D.M., Tsoar, H., and Blumberg, D.G., 2008, A second look at western Sinai seif dunes and their lateral migration: Geomorphology, v. 93, p. 335–342, doi:10.1016/j.geomorph.2007.03.004.
Telfer, M., and Hesse, P., 2013, Palaeoenvironmental reconstructions from linear dunefields: Recent progress, current challenges and future directions: Quaternary Science Reviews, v. 78, p. 1–21, doi:10.1016/j.quascirev.2013.07.007.
Telfer, M.W., 2011, Growth by extension, and reworking, of a south-western Kalahari linear dune: Earth Surface Processes and Landforms, v. 36, p. 1125–1135, doi:10.1002/esp.2140.
Tsoar, H., 1982, Internal structure and surface geometry of longitudinal seif dunes: Journal of Sedimentary Research, v. 52, p. 823–831, doi:10.1306/212F8062-2B24-11D7-8648000102C1865D.
Tsoar, H., 1983, Dynamic processes acting on a longitudinal seif sand dune: Sedimentology, v. 30, p. 567–578, doi:10.1111/j.1365-3091.1983.tb00694.x.
Tsoar, H., 1989, Linear dunes-forms and formation: Progress in Physical Geography, v. 13, p. 507–528, doi:10.1177/030913338901300402.
Tsoar, H., Blumberg, D.G., and Stoler, Y., 2004, Elongation and migration of sand dunes: Geomorphology, v. 57, p. 293–302, doi:10.1016/S0169-555X(03)00161-2.
Ungar, J.E., and Haff, P.K., 1987, Steady state saltation in air: Sedimentology, v. 34, p. 289–299, doi:10.1111/j.1365-3091.1987.tb00778.x.
Vermeesch, P., and Leprince, S., 2012, A 45-year time series of dune mobility indicating constant windiness over the central Sahara: Geophysical Research Letters, v. 39, L14401, doi:10.1029/2012GL052592.
Washington, R., Martin, M.C., Engelstaedter, S., Mbainayel, S., and Mitchell, F., 2006, Dust and the low-level circulation over the Bodélé depression, Chad: Observations from BoDEx 2005: Journal of Geophysical Research, v. 111, D03201, doi:10.1029/2005JD006502.
Wilson, I.G., 1971, Desert sandflow basins and a model for the development of ergs: Geographical Journal, v. 137, p. 180–199, doi:10.2307/1796738.
Zhang, D., Narteau, C., Rozier, O., and Courrech du Pont, S., 2012, Morphology and dynamics of star dunes from numerical modelling: Nature Geoscience, v. 5, p. 463–467, doi:10.1038/ngeo1503.